A ^{99m}Tc-Labeled Ligand of Carbonic Anhydrase IX Selectively Targets Renal Cell Carcinoma In Vivo

Nikolaus Krall*[1], Francesca Pretto*[2], Martin Mattarella[2], Cristina Müller[3], and Dario Neri[1]

[1]*Department of Chemistry and Applied Biosciences, Institute of Pharmaceutical Sciences, ETH Zürich, Zurich, Switzerland;* [2]*Philochem AG, Otelfingen (ZH), Switzerland; and* [3]*Research Department Biology and Chemistry, Paul Scherrer Institut, Center for Radiopharmaceutical Sciences, Villigen-PSI, Switzerland*

Small organic ligands, selective for tumor-associated antigens, are increasingly being considered as alternatives to monoclonal antibodies for the targeted delivery of diagnostic and therapeutic payloads such as radionuclides and drugs into neoplastic masses. We have previously described a novel acetazolamide derivative, a carbonic anhydrase ligand with high affinity for the tumor-associated isoform IX (CAIX), which can transport highly potent cytotoxic drugs into CAIX-expressing solid tumors. The aim of the present study was to quantitatively investigate the biodistribution properties of said ligand and understand whether acetazolamide conjugates merit further development as drug carriers and radioimaging agents. **Methods:** The conjugate described in this study, consisting of a derivative of acetazolamide, a spacer, and a peptidic ^{99m}Tc chelator, was labeled using sodium pertechnetate under reducing conditions and injected intravenously into CAIX-expressing SKRC-52 xenograft–bearing mice. Animals were sacrificed, and organ uptake as percentage injected activity of radiolabeled ligand per gram of tissues (%IA/g) was evaluated between 10 min and 24 h. Additionally, postmortem imaging by SPECT was performed. **Results:** The acetazolamide conjugate described in this study could be labeled to high radiochemical purity (>95%, 2.2–4.5 MBq/nmol). Analysis of organ uptake at various time points revealed that the ligand displayed a maximal tumor accumulation 3 h after intravenous injection (22 %IA/g), with an excellent tumor-to-blood ratio of 70:1 at the same time point. The ligand accumulation in the tumor was more efficient than in any other organ, but a residual uptake in the kidney, lung, and stomach (9, 16, and 10 %IA/g, respectively) was also observed, in line with patterns of carbonic anhydrase isoform expression in those tissues. Interestingly, tumor-to-organ ratios improved on administration of higher doses of radiolabeled ligand, suggesting that certain binding sites in normal organs can be saturated in vivo. **Conclusion:** The ^{99m}Tc-labeled acetazolamide conjugate exhibits high tumor uptake and favorable tumor-to-kidney ratios of up to 3 that may allow imaging of tumors in the kidney and distant sites at earlier time points than commonly possible with antibody-based products. These data suggest that the described molecule merit further development as a radioimaging agent for CAIX-expressing renal cell carcinoma.

Key Words: imaging agent; tumor targeting; kidney cancer; carbonic anhydrase IX

J Nucl Med 2016; 57:943–949
DOI: 10.2967/jnumed.115.170514

Carbonic anhydrase IX (CAIX) is a membrane-bound metalloenzyme involved in the maintenance of cellular acid–base homeostasis. CAIX is virtually undetectable in normal adult organs, with the exception of the stomach, duodenum, bile duct epithelium, and gallbladder (*1,2*). By contrast, the enzyme is strongly expressed in most clear cell renal cell carcinomas (RCCs), as a result of von Hippel–Lindau mutations or deletions (*3*). In addition, CAIX is overexpressed at sites of hypoxia, which are frequently found in neoplastic masses (*4*). CAIX is thus considered to be an attractive target for tumor imaging and targeted drug-delivery applications.

The tumor-homing properties of monoclonal antibodies specific to CAIX have been extensively investigated in quantitative biodistribution studies. One anti-CAIX antibody in IgG format (cG250), labeled with the PET radionuclide ^{124}I, is in advanced clinical development for the detection of metastatic lesions in RCC patients (*5*). However, macromolecular radiotracers, in particular antibodies in IgG format, typically clear slowly from the blood, requiring the use of long-lived radioisotopes and imaging at late time points, which exposes patients to a high radiation burden (*6*). Indeed, ^{124}I-cG250 only reaches tumor-to-blood ratios suitable for imaging 2–7 d after injection into the patient.

Dubois et al. first proposed the use of radiolabeled small organic CAIX ligands for tumor imaging applications (*7*). Unlike large macromolecules, small molecules clear rapidly from circulation and thus reach tumor-to-blood ratios suitable for imaging at early time points (*8–10*). This in turn permits the use of radioisotopes with shorter half-lives, reduces the radiation burden to the patient, and allows physicians to obtain diagnostic information much more quickly than with antibody-based imaging agents.

Despite the potential advantages of small-molecule CAIX ligands for tumor imaging applications, the development of small-molecule radiotracers for CAIX-expressing solid tumors has so far remained elusive. Quantitative biodistribution studies of the radiolabeled small organic CAIX ligand VM4-037 exhibited poor uptake in the tumor and strong accumulation in the kidney, ileum, colon, liver, stomach, and bladder in mice (*11*). Strong kidney and liver uptake with little clearance over the study period was also observed in healthy human

Received Nov. 30, 2015; revision accepted Feb. 4, 2016.
For correspondence or reprints contact: Dario Neri, IPW, D-CHAB, ETH Zürich, Vladimir-Prelog-Weg 1-5/10, 8093 Zurich, Switzerland.
E-mail: neri@pharma.ethz.ch
*Contributed equally to this work.
Published online Feb. 18, 2016.

volunteers (*12*). Similar results were obtained with ^{99m}Tc-labeled derivatives of phenylsulfonamide in mice (*13*).

Our group and Claudiu Supuran have previously shown that high-affinity small organic ligands of CAIX not only efficiently localize to RCC tumors in mouse models when labeled with a fluorescent dye, but also can be used for the selective delivery of cytotoxic agents into CAIX-expressing solid tumors, with encouraging therapeutic results (*14,15*). The affinity of CAIX ligands appears to correlate with the in vivo tumor-targeting performance.

Here, we describe the synthesis of an acetazolamide (AAZ)-based carbonic anhydrase ligand with high affinity for the tumor-associated isoform CAIX, labeled with ^{99m}Tc, a widely used γ-emitting radionuclide for nuclear medicine applications. The ligand exhibited favorable biodistribution profiles in CAIX-expressing tumor-bearing mice, with excellent tumor-to-organ (up to 3 for tumor over kidney) and tumor-to-blood ratios (>100), already a few hours after intravenous administration. The high selectivity exhibited by this small-molecule CAIX ligand reinforces the concept that small organic ligands, endowed with sufficient affinity to good-quality tumor-associated antigens, may be considered as a valuable alternative to monoclonal antibodies and antibody fragments for tumor imaging (*8,16*) and drug-delivery applications. Indeed, we hope to ultimately develop the described molecule into a clinically validated radiotracer for the detection of CAIX-expressing RCC.

MATERIALS AND METHODS

Synthesis

General Procedure for Solid-Phase Peptide Synthesis. Prior to the first coupling step, chlorotrityl resin (500 mg; RAPP Polymers) preloaded with Fmoc-Cys(Trt)-OH was placed inside a syringe equipped with a filter pad for solid-phase synthesis and swollen with dimethylformamide (DMF, 10 mL) for 15 min. Fmoc deprotection was achieved by shaking the resin with 20% v/v piperidine in DMF (5 mL) for 1 min followed by two more rounds with fresh 20% v/v piperidine solution in DMF (5 mL) for 10 min each. After deprotection, the resin was washed with DMF (3 × 8 mL). Amino acids were coupled by mixing the Fmoc-protected acid (3 equivalents) with 2-(1H-benzotriazol-1-yl)-1,1,3,3-tetramethyluronium hexafluorophosphate (ChemPep, 3 equivalents), hydroxybenzotriazole (ChemPep, 3 equivalents), and DIPEA (Sigma Aldrich, 6 equivalents) in DMF (5 mL). The solution was allowed to react with the resin for 1 h and was discarded and the resin washed with DMF (3 × 8 mL). Coupling and deprotection steps were alternated until the desired peptide had been synthesized.

Synthesis of ^{99m}Tc-Chelating AAZ Derivative 1. In consecutive order the following Fmoc-protected amino acids were coupled to Fmoc-Cys (Trt)-OH preloaded chlorotrityl resin: Fmoc-Asp(OtBu)-OH, Boc-Lys (Fmoc)-OH, and Fmoc-Asp(OtBu)-OH (Sigma Aldrich). After the final deprotection, the resin was capped with 5-azido pentanoic acid (ChemPep) using the general coupling procedure. The targeting ligand was installed by reacting the resin with a solution of CuI (ABCR, 0.1 equivalent), Tris(benzyltriazolylmethyl)amine (TBTA, (*17*), 0.1 equivalent), and *N*-(5-sulfamoyl-1,3,4-thiadiazol-2-yl)hex-5-ynamide ((*15*), 2 equivalents) in DMF (2.5 mL) and THF (2.5 mL) for 12 h. The resin was washed with DMF (3 × 8 mL), an aqueous solution of ethylenediaminetetraacetate (EDTA) in H_2O (50 mM, 3 × 8 mL), H_2O (3 × 8 mL), MeOH (3 × 8 mL), and dichloromethane (DCM, 3 × 8 mL). For peptide cleavage and deprotection, the resin was suspended in an ice-cold mixture of trifluoroacetic acid (TFA; Sigma Aldrich, 7 mL), thioanisole (Sigma Aldrich, 320 μL), *m*-cresol (Sigma Aldrich, 320 μL), H_2O (160 μL), and triisopropylsilane (TIS; Sigma Aldrich, 160 μL). After 1 h, the deprotection solution was added drop-wise to ice-cold Et_2O (150 mL) and the precipitate isolated by filtration. The crude product was dissolved in 1:1 v/v H_2O, MeCN and lyophilized to yield an off-white powder (560 mg crude). Aliquots of the crude product (4 × 50 mg) were dissolved in dimethylsulfoxide (DMSO, 4 × 900 μL), 2-thioethanol (Sigma Aldrich, 4x 100 μL) was added, and the crude product was purified over reversed-phase high-performance liquid chromatography (HPLC) (40 runs; Synergi RP Polar; 5% MeCN in 0.1% aqueous TFA to 80% MeCN over 20 min). Fractions containing the desired product as indicated by low-resolution mass spectrometry were pooled and lyophilized to give the product as a white powder (19.1 mg).

^{1}H-NMR (500 MHz, DMSO-*d6*) δ [ppm] = 12.99 (s, 1H), 8.73 (d, J = 7.4 Hz, 1H), 8.37 (s, 2H), 8.25 (d, J = 7.9 Hz, 1H), 8.09–0.07 (m, 4H), 7.87 (s, 1H), 7.81 (t, J = 5.7 Hz, 1H), 4.69–4.66 (m, 1H), 4.54–4.50 (m, 1H), 4.43–4.40 (m, 1H), 4.30 (t, J = 7.0 Hz, 2H), 3.75–3.74 (m, superimposed with water peak), 3.05–2.98 (m, 3H), 2.90–2.55 (m, 10H), 2.48–2.37 (m, 2H), 2.15 (t, J = 7.3 Hz, 2H), 1.99–1.93 (m, 2H), 1.81–1.68 (m, 4H), 1.48–1.25 (m, 6H); HRMS (m/z) $[M+H]^+$ calculated for $C_{30}H_{47}N_{12}O_{13}S_3$ 879.2542; found 879.2539.

Synthesis of ^{99m}Tc-Chelating Derivative 2. In consecutive order the following Fmoc-protected amino acids were coupled to Fmoc-Cys (Trt)-OH preloaded chlorotrityl resin: Fmoc-Asp(OtBu)-OH, Boc-Lys (Fmoc)-OH and Fmoc-Asp(OtBu)-OH (Sigma Aldrich). After the final deprotection, the resin was capped with 5-azido pentanoic acid (ChemPep) using the general coupling procedure. The targeting ligand was installed by reacting the resin with a solution of CuI (ABCR, 0.1 equivalents), TBTA ((*17*), 0.1 equivalent), and hex-5-ynamide (Sigma Aldrich, 2 equivalents) in DMF (2.5 mL) and THF (2.5 mL) for 12 h. The resin was washed with DMF (3 × 8 mL), an aqueous solution of EDTA in H_2O (50 mM, 3 × 8 mL), H_2O (3 × 8 mL), MeOH (3 × 8 mL), and DCM (3 × 8 mL). For peptide cleavage and deprotection, the resin was suspended in an ice-cold mixture of TFA (7 mL), thioanisole (320 μL), m-cresol (320 μL), H_2O (160 μL), and TIS (160 μL). After 1 h, the deprotection solution was added drop-wise to ice-cold Et_2O (150 mL) and the precipitate isolated by filtration. The crude product was dissolved in 1:1 v/v H_2O, MeCN and lyophilized to yield an off-white powder (650 mg crude). Aliquots of the crude product (4 × 50 mg) were dissolved in DMSO (4 × 900 μL), 2-thioethanol (4 × 100 μL) was added, and the crude product was purified over reversed-phase HPLC (40 runs, Synergi RP Polar, 5% MeCN in 0.1% aqueous TFA to 80% MeCN over 20 min). Fractions containing the desired product as indicated by low-resolution mass spectrometry were pooled and lyophilized to give the product as a white powder (35 mg).

^{1}H-NMR (500 MHz, DMSO-*d6*) δ [ppm] = 8.74 (d, J = 5.07 Hz, 1H), 8.25 (d, J = 7.85 Hz, 1H), 8.09–8.07 (4H), 7.83 (s, 1H), 7.81 (t, J = 5.6 Hz, 1H), 7.26 (s, 1H), 6.74 (s, 1H), 4.70–4.66 (m, 1H), 4.54–4.49 (m, 1H), 4.43–4.40 (m, 1H), 4.29 (t, J = 7.0 Hz, 2H), 3.74 (br s, 2H), 3.07–2.95 (m, 2H), 2.90–2.86 (m, 1H), 2.82–2.55 (m, 6H), 2.48–2.37 (m, 2H), 2.15 (t, J = 7.3 Hz, 2H), 2.10 (t, J = 7.5 Hz, 2H), 1.83–1.68 (m, 6H), 1.47–1.25 (m, 6H); HRMS (m/z) $[M+H]^+$ calculated for $C_{28}H_{46}N_9O_{11}S$ 716.3032; found 716.3020.

Stability

Incubation of Radiolabeled Preparations in Serum and Whole Blood. The ability of AAZ-based CAIX binder to interact with blood cells was determined by a centrifugation-based assay with radiolabeled preparation. ^{99m}Tc-labeled preparations were incubated at the final concentration of 10 μg/mL in fresh blood collected via cardiac puncture from mice at sacrifice in microtainer LH tubes (BD). After mixing or following 10 min of incubation, tubes were centrifuged (2,000*g*, 3 min) and plasma was separated from the cell pellet. To separate the protein fraction from the soluble fraction 1 volume of acetonitrile (Sigma) was added to 1 volume of solution; the mixture was shaken for 30 s and centrifuged (8,000*g*, 4 min).

The stability of ^{99m}Tc-labeled preparations was analyzed in mouse serum (Sigma-Aldrich) at the final concentration of 10 μg/mL. After mixing or following 10 min, 30 min, 1 h, or 3 h of incubation, the protein fraction was separated following the procedure reported above.

The radioactivity of isolated cell fractions, soluble fractions, and protein fractions were recorded using a Packard Cobra γ-counter. Results are represented as percentages over the total amount of measured radioactivity.

Surface Plasmon Resonance. Surface plasmon resonance experiments were carried out at room temperature (25°C) using a Biacore S200 instrument and CM5 chips (GE Healthcare). For all measurements, phosphate-buffered saline (PBS) (pH 7.4) containing DMSO (5% v/v) was used. CAIX and CAII solution in acetate buffer (500 nM, pH 5.0) were immobilized on the chip at about 1,500 response units using ethylcarbodiimide hydrochloride and *N*-hydroxysuccinimide as described by the instrument manufacturer. The sensograms were measured for solutions in PBS (pH 7.4) containing DMSO (5% v/v) of compound 1 and reference AAZ at a concentration of 40 nM. Sensograms were solvent-corrected with the Biacore S200 evaluation software. (Supplemental Figs. 1–5 [supplemental materials are available at http://jnm.snmjournals.org].)

Radiolabeling

^{99m}Tc ligand conjugate (60 nmol) in PBS (pH 7.4; 50 μL) was mixed with $SnCl_2$ (Sigma Aldrich, 200 μg) and sodium glucoheptonate (TCI, 20 mg) in H_2O (150 μL). Tris-buffered saline (pH 7.4; 600 μL) was added and the solution degassed thoroughly by bubbling it with N_2 for 5 min. Na$^{99m}TcO_4$-generator eluate (200 μL, 135–276 MBq; Mallinckrodt) was added and the reaction mixture heated to 90°C for 20 min. After being cooled to room temperature, an aliquot was analyzed by RP-HPLC (XTerra C18, 5% MeCN in 0.1% aqueous trifluoroacetic acid to 80% over 20 min on a Merck-Hitachi D-7000 HPLC system equipped with a Raytest Gabi Star radiodetector). Radiolabel incorporations greater than 95% were routinely achieved. The labeling solution was then diluted to the desired injection concentration with PBS and assayed for stability at different time points using RP-HPLC as described above. Activities used are listed in Supplemental Table 1.

Cell Culture, Animal, and Tumor Model

The human RCC cell line SKRC-52 was a kind gift from Professor Egbert. Oosterwijk (Radboud University Nijmegen Medical Centre). On thawing, cells were kept in culture for no longer than 10 passages. The SKRC-52 cell line was periodically authenticated by morphologic inspection and tested negative for *Mycoplasma* contamination by polymerase chain reaction tests in 2014–2015. SKRC-52 cells were maintained in RPMI medium (Invitrogen) supplemented with 10% heat-inactivated fetal calf serum (Gibco) in a humidified atmosphere with 5% CO_2 at 37°C. For passaging, cells were detached using trypsin with ethylenediaminetetraacetic acid 0.05% (Gibco). Exponentially growing cells were harvested, repeatedly washed, counted, and resuspended in PBS, pH 7.4, before injection.

SKRC-52 cells (5×10^6 cells) were transplanted subcutaneously in the flank of athymic BALB/c *nu/nu* mice (age, 8–10 wk; Charles River). Tumor growth was monitored with the aid of a digital caliper (volumes were measured with the following formula: length (mm) × width^2 (mm^2)/2. All animal experiments were conducted in accordance with Swiss animal welfare laws and regulations and approved by Veterinaeramt des Kanton Zurich.

Quantitative Biodistribution Studies

SKRC-52 tumor–bearing mice ($n = 3$ mice per group) were randomized on the basis of tumor volume and injected intravenously with radiolabeled preparations. Ten minutes, 1 h, 3 h, 6 h, and 24 h after the injection, mice were sacrificed and organs collected and weighed and radioactivity measured with a Packard Cobra γ-counter. Values were decay-corrected and expressed as percentage injected activity per gram (%IA/g) ± SD.

SPECT

SPECT/CT images were acquired 4 h after the injection of ^{99m}Tc-1 (0.17 MBq) with a 4-head multiplexing multipinhole small-animal SPECT camera (NanoSPECT/CT; Mediso Medical Imaging Systems). Total acquisition time was 9 h. The energy peak for the camera was set at 140.5 keV ± 10%. The SPECT images were acquired with Nucline Software (version 1.02; Bioscan Inc.), and data were reconstructed with HiSPECT software (version 1.4.3049; Scivis GmbH). The images were prepared using the VivoQuant postprocessing software (version 1.23; inviCRO Imaging Services and Software).

RESULTS

A novel CAIX ligand, containing AAZ as a targeting moiety, a triazine-based linker, and a Lys-Asp-Cys-based moiety for ^{99m}Tc chelation (compound 1), was synthesized according to the scheme depicted in Figure 1 and subjected to standard chemical characterization (Supplemental Figs. 1–5). A structurally related compound 2, devoid of the AAZ moiety, was used as negative control (Fig. 1B). An optimized labeling procedure routinely allowed an incorporation of ^{99m}Tc greater than 95% (2.2–4.5 MBq/nmol), giving products of excellent radiochemical purity (Fig. 1D) and ready for use without further purification (Supplemental Figs. 6 and 7 demonstrate for stability).

Unlabeled 1 exhibited binding to recombinant CAIX extracellular domain as measured by surface plasmon resonance (Supplemental Fig. 8) that was comparable to the approved antiglaucoma drug AAZ from which it was originally derived. Because AAZ is a pan-CA ligand with broad isoform selectivity, we also tested the binding capacity of 1 toward the ubiquitous isoform CAII isolated from erythrocytes and found an interaction comparable to AAZ (Supplemental Fig. 8). However, because 1 is large and multiply charged we expected it to be membrane-impermeable and to not interact with intracellular CAs that make up most CA isoforms in humans. Indeed, binding of radiolabeled 1 to HEK cells was dependent on the ectopic expression of CAIX (Supplemental Fig. 9). These findings are in line with previously obtained results in which derivatives of 1 had been shown to be portable ligands of CAIX with low nanomolar affinity whereas derivatives of 2 were suitable nonbinding negative controls (*14,15*).

Mice with subcutaneously grafted human RCC, derived from the human cell line SKRC-52, were used to assess the tumor-targeting properties of the novel radiotracer. Several CAIX-expressing xenograft models of human RCC have been studied for tumor-targeting application directed against CAIX in the past. SKRC-52 tumors consistently exhibited the lowest uptake of anti-CAIX monoclonal antibodies (*18–20*) and were chosen as the most challenging yet validated model available. Radiolabeled compounds 1 and 2 were injected into the tail vein, initially at a mass amount of 13 μg/kg (corresponding to 14 nmol/kg for 1 and 17 nmol/kg for 2) and an activity of 1.4 and 0.9 MBq, respectively. Mice were sacrificed at various time points, organs were collected, and radioactivity was counted, allowing the expression of biodistribution results as %IA/g. Three hours after injection, a maximum of 22 %IA/g of the radiolabeled product accumulated in the tumor. Tumor-to-blood ratios peaked 6 h after injection, with excellent selectivity (~100, Fig. 2A; Supplemental Fig. 10; Supplemental Table 2). Tumor-to-organ ratios were also favorable for spleen

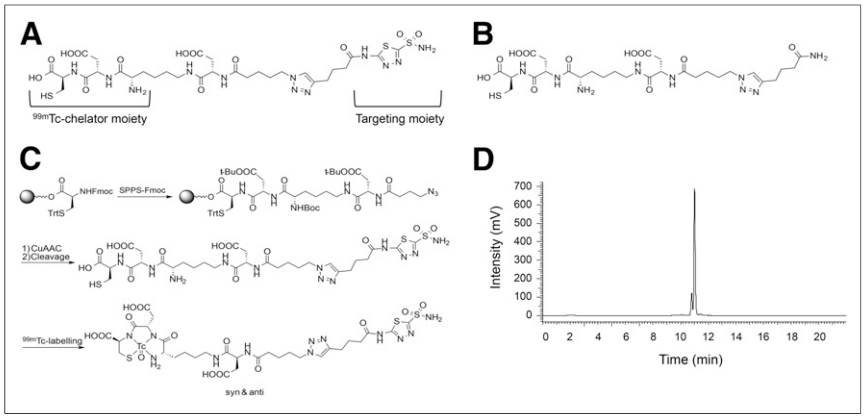

FIGURE 1. (A) Structure of tumor-targeting ligand chelator conjugate 1. Targeting moiety is derived from approved antiglaucoma drug AAZ and has previously been shown to tolerate attachment to diverse payloads including fluorophores and drugs while maintaining low nanomolar affinity for CAIX. Peptidic ^{99m}Tc chelator moiety has previously been shown to be suitable for imaging applications in mice and humans. (B) Structure of negative control compound 2 lacking a CAIX-binding ligand. (C) Synthesis of the CAIX-binding ligand chelator conjugate by solid-phase peptide synthesis. Peptide backbone was constructed using standard Fmoc chemistry. Targeting ligand was installed using copper-catalyzed azide-alkyne cycloaddition. Radiolabeling was achieved with ^{99m}Tc-pertechnetate under reducing conditions. (D) Representative radiochromatogram of labeled ligand chelator conjugate 1. Please note 2 diastereomers resulting from labeling procedure (*syn* and *anti*) that can be separated chromatographically.

(141) and heart (13.9) at the same time point. Lower selectivity was observed for other organs, with tumor-to-liver, tumor-to-lung, tumor-to-kidney, tumor-to-intestine, and tumor-to-stomach ratios of 4.7, 2.1, 1.5, 5.1 and 4.0 at 6 h, that increased to 15, 6.2, 2.5, 10.4, and 6.4 at 24 h, respectively. The nature of the injection buffer (Tris-buffered saline vs. PBS) did not strongly influence biodistribution results (Supplemental Fig. 11). By contrast, a ^{99m}Tc-labeled preparation of compound 2 (serving as negative control) failed to exhibit a preferential accumulation at the tumor site (Fig. 2B). Similarly, free $Na^{99m}TcO_4$ did not preferentially accumulate inside the tumor (Supplemental Fig. 12).

To learn more about the dependence of biodistribution profiles on the injected tracer dose of compound 1, we studied biodistribution profiles 6 h after intravenous administration of the ^{99m}Tc-labeled compound at doses ranging between 2.5 and 65 μg/kg (2.8 and 74 nmol/kg). In addition, we investigated the effect of a preinjection of a nonradioactive dose of the compound 1, followed 10 min later by the administration of the labeled compound (i.e., 40 + 40 μg/kg [45 + 45 nmol/kg] or 200 + 40 μg/kg [227 + 45 nmol/kg], Fig. 3; Supplemental Table 3). In this case, the quantification of organ distribution was performed 3 h after the administration of the radiolabeled preparation. The best biodistribution profiles were observed in the range between 25 and 80 μg/kg (28 and 90 nmol/kg). Tumor-to-organ ratios 6 h after injection of a 25 μg/kg (28 nmol/kg) dose were 2.9, 4.9, 5.8, 10.3, 14.9, 109, and 26.9 for kidney, lung, liver, stomach, intestine, spleen, and heart, respectively.

To test the suitability of 1 to detect CAIX-expressing RCC tumors in vivo, we intravenously injected 10 μg/kg (11 nmol/kg) of radiolabeled 1 into the SKRC-52 xenograft mouse model of human RCC and subjected it to SPECT/CT. As expected from the quantitative biodistribution data, radioactivity strongly accumulated inside the tumor, with a visibly higher accumulation inside the RCC xenograft relative to kidneys (Fig. 4).

DISCUSSION

Tumor imaging and drug-delivery applications crucially rely on the availability of ligands, which strongly and selectively localize at the site of disease. A high binding affinity to an accessible target, which is expressed abundantly and selectively in the tumor environment, represents an essential prerequisite for efficient tumor accumulation (*16*). Typically, monoclonal antibodies have been considered as the ligands of choice for most tumor-targeting applications. However, it is now becoming increasingly clear, that high-affinity small-molecule ligands of extracellular tumor–associated antigens may offer several advantages over tumor-homing monoclonal antibodies (*8*). For example, antibodies, in particular in IgG format, have slow blood clearance kinetics (*21*) and may only slowly and inefficiently penetrate into solid tumors (*22*). In the context of nuclear medicine applications, this requires the use of long-lived radioisotopes and imaging at late time points, which exposes patients to a high radiation burden (*5*). Additionally, monoclonal antibodies may be immunogenic, which can preclude repeated administration for routine diagnostic procedures (*23*). Most small molecules, on the other hand, exhibit fast blood clearance and tumor-targeting kinetics and are typically not immunogenic (*8*).

In the present study, we investigated 1 as a potential novel small-molecule radiotracer for the detection of CAIX-expressing RCC in a preclinical mouse model of the disease. CAIX is a well-studied tumor antigen that is strongly expressed in most RCCs and has previously been validated for antibody-based imaging and targeted drug-delivery applications (*18–20*). Despite this fact, the development of small-molecule radiotracers that strongly and selectively accumulate inside CAIX-expressing RCCs has so far remained elusive (*11*).

Radiotracer 1 contains a high-affinity CAIX-binding moiety derived from the approved antiglaucoma drug AAZ connected to an efficient ^{99m}Tc chelator that has previously been used in animals and humans (*24,25*). Labeling was achieved with high radiochemical purity (>95%, 2.2–4.5 MBq/nmol). The presence of 2 distinct labeled species can be attributed to the existence of *syn* and *anti* diastereomers arising from 2 binding orientations of the chiral ^{99m}Tc ligand with respect to ^{99m}Tc-O bond (*24*). The precursor of 1 was diastereomerically pure as shown by nuclear magnetic resonance.

On injection of ^{99m}Tc-labeled 1 into SKRC-52 CAIX-expressing xenograft-bearing mice, the ligand strongly accumulated in the target lesion and was excreted rapidly from blood and other healthy organs, achieving a tumor-to-blood ratio of 70 after only 3 h and up to 100 after 6 h. ^{124}I-labeled cG250 antibody, on the other hand, achieved a tumor-to-blood ratio of less than 2 at 72 h after administration to SKRC-52 xenograft–bearing mice (*19*) whereas absolute tumor accumulation of 1 was comparable to the antibody (~20 %IA/g). Interestingly, absolute uptake of 1 in the tumor peaked after 3 h (22 %IA/g) although the ligand had

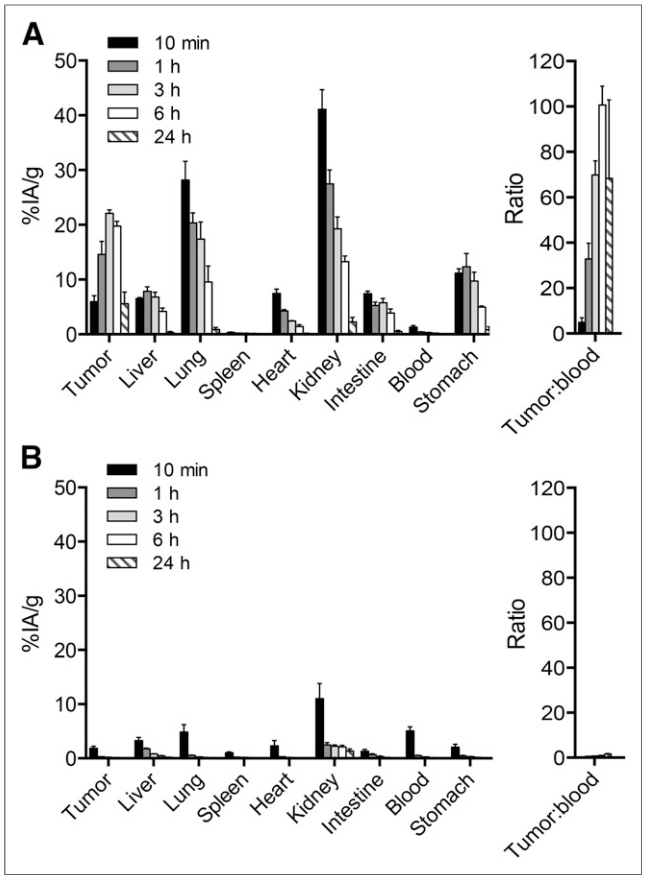

FIGURE 2. (A) Quantitative biodistribution of radiolabeled CAIX-binding ligand chelator conjugate 1 at different time points after intravenous injection (13 μg/kg, 14 nmol/kg). Ligand accumulates in tumor, reaching maximum uptake values after 3 h. Tumor-to-blood ratios are high (70:1) after 3 h already and further increase to 100:1 after 6 h. (B) Quantitative biodistribution of radiolabeled negative control compound 2 lacking CAIX-binding moiety at different time points after intravenous injection (13 μg/kg, 17 nmol/kg). Radioconjugate lacking tumor-antigen-binding moiety does not achieve a strong uptake inside tumor.

almost completely cleared from blood 1 h after injection already. This suggests that a pool of labeled 1 exists outside the bloodstream (e.g., in interstitial fluid) that slowly accumulates in the tumor over time when blood pools have already cleared through the kidneys.

Higher absolute tumor accumulations than with ^{124}I-cG250 and 1 have previously been reported with ^{111}In-labeled cG250 and ^{89}Zr-labeled cG250 in the SKRC-52 xenograft model (60 and 49 %IA/g), presumably due to the residualizing nature of the radioisotope. Although ^{111}In-cG250 also suffered from low tumor-to-blood ratios (~6), ^{89}Zr-cG250 achieved almost twice that selectivity (~11) albeit only after 7 d after injection (*19,20*). At the same time, 2 antibodies previously raised in our own laboratory against recombinant CAIX extracellular domain using phage display exhibited high-binding-affinity CAIX in vitro (equilibrium dissociation constant = 2.4 and 3.2 nM for the scFv) and selectively stained the antigen in tissue-thin sections but failed to strongly accumulate inside CAIX-expressing tumors after intravenous injection (*26*). These discrepancies are so far not understood but may relate to different epitopes bound by the antibodies.

Although AAZ derivative 1 exhibited favorable tumor-to-blood ratios and tumor-to-organ ratios for some normal organs (e.g., spleen, heart), a nonnegligible uptake in the kidney, stomach, intestine, and lung was observed in biodistribution studies. CAIX is indeed strongly expressed in stomach and in certain intestinal structures (*1,2*). Moreover, other carbonic anhydrase isoforms are expressed on the cell surface in the kidney and lung (*27*). Interestingly, we found that the use of higher doses of CAIX ligands yielded the best in vivo selectivities, suggesting that binding sites in normal organs may be saturated in vivo at suitable doses, whereas free receptors are still available on tumor cells.

Uptake in most healthy organs achieved by 1 were comparable to those previously published for cG250 (e.g., in lung depending on the dose 1–5 %IA/g for 1; 5 %IA/g for ^{124}I- and ^{111}In-labeled cG250). Deviations between the antibody and small molecule may be attributed to differences in ligand specificity, labeling strategy, or target accessibility. Indeed, tissue uptake can be a function of exact antigen location, degree of vascularization, and vascular permeability (*19,28*). The most striking difference in normal organ uptake was observed for the kidney. Radiolabeled cG250 consistently exhibited a higher tumor-to-kidney ratio than 1, with values as high as 10 being possible, albeit at the cost of longer plasma circulation times. Antibodies in IgG format are larger than the renal filtration threshold (*29*) and therefore cannot reach antigens in the proximal tubules. Radiotracer 1 on the other hand is filtered through the kidneys and can potentially bind extracellular carbonic anhydrases expressed in kidneys.

Nevertheless, tumor-to-kidney ratios of up to 3 were achieved with 1, which appear to surpass those previously reported for other small organic ligands (e.g., folate derivatives, urea derivatives of glutamic acid for prostate-specific membrane antigen targeting). Both ligands are being investigated for imaging of the targeted tumor delivery of therapeutic radionuclides or of cytotoxic drugs (*24,30*). Importantly, a tumor-to-kidney ratio of 3 is expected to be sufficient even for the detection of primary kidney lesions against kidney background. This view was further supported by SPECT/

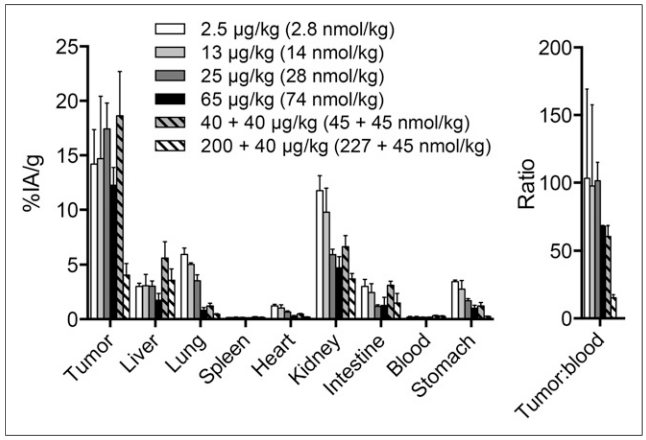

FIGURE 3. (A) Quantitative biodistribution analysis of radiolabeled CAIX-binding ligand chelator conjugate 1 6 h (solid fills) or 3 h (striped fills) after intravenous injection of different doses. Solid fills correspond to 2.5–65 μg/kg (28–74 nmol/kg). Striped fills correspond to 40 (45 nmol/kg) or 200 μg/kg (227 nmol/kg) of unlabeled followed after 10 min by 40 μg/kg (45 nmol/kg) of labeled conjugate. Doses of 25–65 μg/kg (28–74 nmol/kg) of labeled conjugate or 40 μg/kg (45 nmol/kg) of unlabeled followed by equal dose of labeled conjugate give excellent tumor uptake and tumor-to-organ ratios.

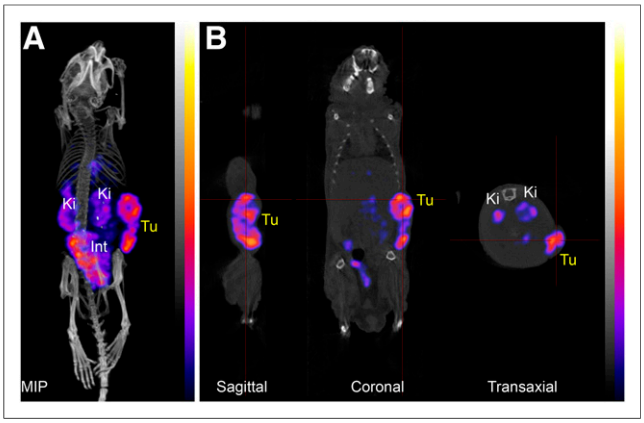

FIGURE 4. SPECT/CT scan 4 h after injection of radiolabeled 1 (10 μg/kg, 11 nmol/kg, 0.17 MBq) into a SKRC-52 xenograft–bearing mouse. Maximum-intensity projection (MIP) (A) and sagittal, coronal, and transaxial projections (B) through SKRC-52 xenograft tumor implanted on right flank. Int = intestine; Ki = kidney; Tu = tumor.

CT data demonstrating a clearly visible high tumor uptake against a lower kidney background.

The encouraging biodistribution properties of this novel radiotracer warrant future clinical investigations for the detection of CAIX-positive lesions in patients. The rapid clearance profile of the ligand and the favorable physical properties of ^{99m}Tc should facilitate molecular imaging applications with reduced radiation burden to patients, compared with the ^{124}I-labeled cG250 antibody, which is currently in clinical development programs (*5*). Favorable biodistribution studies have also been reported for a 2-step pretargeting strategy, featuring the administration of a trispecific antibody against CAIX and a metal chelator, followed by the administration of a homobivalent chelator-radiometal complex (*28*). This approach, however, may be difficult to routinely implement in the clinic.

Radiolabeled AAZ-based compound 1 may also serve as a companion imaging agent for small ligand–based drug-delivery strategies using AAZ derivatives coupled to potent cytotoxic drugs (such as DM1 or monomethyl auristatin E (*14,15,31*)). It is becoming increasingly clear that small-molecule targeting agents may also represent an alternative to antibodies for the delivery of anticancer drugs into solid tumors, helping spare normal organs (*8,16*). Indeed, radiotracer 1 exhibited better uptake in subcutaneous SKRC-52 xenografts than typically achieved by standard chemotherapeutic drugs in different xenograft models (Supplemental Fig. 13).

CONCLUSION

Collectively, our data suggest that AAZ derivatives are attractive ligands for the targeted delivery of radionuclides into CAIX-expressing solid tumors. AAZ derivatives in conjugate with different radiometal chelators may be used as imaging agents for the detection of CAIX-expressing tumors in patients but potentially also for the therapeutic delivery of β-emitting radionuclides or of anticancer drugs to patients with CAIX-positive tumors. We are currently planning dosimetric studies with 1 in patients with RCC, to understand if imaging agents and drug-delivery strategies based on AAZ-like ligands merit further development for use in human RCC patients.

DISCLOSURE

The costs of publication of this article were defrayed in part by the payment of page charges. Therefore, and solely to indicate this fact, this article is hereby marked "advertisement" in accordance with 18 USC section 1734. This work was supported by ETH Zürich, the Swiss National Science Foundation (SNSF), Philochem AG, and Kommission fur Technologie und Innovation (KTI 17072.1 PFLS-LS). Dario Neri is cofounder and President of the Scientific Advisory Board of Philogen SpA and Philochem AG, who have obtained an exclusive license for the commercial development of described radio ligand and derivatives. Nikolaus Krall is entitled to licensing revenues from a patent describing the ligand presented in this study. No other potential conflict of interest relevant to this article was reported.

ACKNOWLEDGMENTS

We thank Sarah Wulhfard for the help with experimental work and for helpful discussion.

REFERENCES

1. Saarnio J, Parkkila S, Parkkila AK, et al. Immunohistochemistry of carbonic anhydrase isozyme IX (MN/CA IX) in human gut reveals polarized expression in the epithelial cells with the highest proliferative capacity. *J Histochem Cytochem.* 1998;46:497–504.
2. Karhumaa P, Kaunisto K, Parkkila S, et al. Expression of the transmembrane carbonic anhydrases, CA IX and CA XII, in the human male excurrent ducts. *Mol Hum Reprod.* 2001;7:611–616.
3. Bui MH, Seligson D, Han KR, et al. Carbonic anhydrase IX is an independent predictor of survival in advanced renal clear cell carcinoma: implications for prognosis and therapy. *Clin Cancer Res.* 2003;9:802–811.
4. Ivanov S, Liao SY, Ivanova A, et al. Expression of hypoxia-inducible cell-surface transmembrane carbonic anhydrases in human cancer. *Am J Pathol.* 2001;158:905–919.
5. Divgi CR, Pandit-Taskar N, Jungbluth AA, et al. Preoperative characterisation of clear-cell renal carcinoma using iodine-124-labelled antibody chimeric G250 (^{124}I-cG250) and PET in patients with renal masses: a phase I trial. *Lancet Oncol.* 2007;8:304–310.
6. Divgi CR, Uzzo RG, Gatsonis C, et al. Positron emission tomography/computed tomography identification of clear cell renal cell carcinoma: results from the REDECT trial. *J Clin Oncol.* 2013;31:187–194.
7. Dubois L, Lieuwes NG, Maresca A, et al. Imaging of CA IX with fluorescent labelled sulfonamides distinguishes hypoxic and (re)-oxygenated cells in a xenograft tumour model. *Radiother Oncol.* 2009;92:423–428.
8. Krall N, Scheuermann J, Neri D. Small targeted cytotoxics: current state and promises from DNA-encoded chemical libraries. *Angew Chem Int Ed Engl.* 2013;52:1384–1402.
9. Barrett JA, Coleman RE, Goldsmith SJ, et al. First-in-man evaluation of 2 high-affinity PSMA-avid small molecules for imaging prostate cancer. *J Nucl Med.* 2013;54:380–387.
10. Fisher RE, Siegel BA, Edell SL, et al. Exploratory study of ^{99m}Tc-EC20 imaging for identifying patients with folate receptor-positive solid tumors. *J Nucl Med.* 2008;49:899–906.
11. Peeters SG, Dubois L, Lieuwes NG, et al. [F]VM4-037 MicroPET imaging and biodistribution of two in vivo CAIX-expressing tumor models. *Mol Imaging Biol.* 2015;17:615–619.
12. Doss M, Kolb HC, Walsh JC, et al. Biodistribution and radiation dosimetry of the carbonic anhydrase IX imaging agent [^{18}F]VM4-037 determined from PET/CT scans in healthy volunteers. *Mol Imaging Biol.* 2014;16:739–746.
13. Akurathi V, Dubois L, Celen S, et al. Development and biological evaluation of ^{99m}Tc-sulfonamide derivatives for in vivo visualization of CA IX as surrogate tumor hypoxia markers. *Eur J Med Chem.* 2014;71:374–384.
14. Krall N, Pretto F, Neri D. A bivalent small molecule-drug conjugate directed against carbonic anhydrase IX can elicit complete tumour regression in mice. *Chem Sci (Camb).* 2014;5:3640–3644.

15. Krall N, Pretto F, Decurtins W, Bernardes GJ, Supuran CT, Neri D. A small-molecule drug conjugate for the treatment of carbonic anhydrase IX expressing tumors. *Angew Chem Int Ed Engl.* 2014;53:4231–4235.
16. Srinivasarao M, Galliford CV, Low PS. Principles in the design of ligand-targeted cancer therapeutics and imaging agents. *Nat Rev Drug Discov.* 2015;14:203–219.
17. Chan TR, Hilgraf R, Sharpless KB, Fokin VV. Polytriazoles as copper(I)-stabilizing ligands in catalysis. *Org Lett.* 2004;6:2853–2855.
18. Kranenborg MH, Boerman OC, de Weijert MC, Oosterwijk-Wakka JC, Corstens FH, Oosterwijk E. The effect of antibody protein dose of anti-renal cell carcinoma monoclonal antibodies in nude mice with renal cell carcinoma xenografts. *Cancer.* 1997;80:2390–2397.
19. van Schaijk FG, Oosterwijk E, Molkenboer-Kuenen JD, et al. Pretargeting with bispecific anti-renal cell carcinoma x anti-DTPA(In) antibody in 3 RCC models. *J Nucl Med.* 2005;46:495–501.
20. Stillebroer AB, Franssen GM, Mulders PFA, et al. ImmunoPET imaging of renal cell carcinoma with I-124- and Zr-89-labeled anti-CAIX monoclonal antibody cG250 in mice. *Cancer Biother Radiopharm.* 2013;28:510–515.
21. Borsi L, Balza E, Bestagno M, et al. Selective targeting of tumoral vasculature: comparison of different formats of an antibody (L19) to the ED-B domain of fibronectin. *Int J Cancer.* 2002;102:75–85.
22. Dennis MS, Jin H, Dugger D, et al. Imaging tumors with an albumin-binding Fab, a novel tumor-targeting agent. *Cancer Res.* 2007;67:254–261.
23. Brüggemann M, Winter G, Waldmann H, Neuberger MS. The immunogenicity of chimeric antibodies. *J Exp Med.* 1989;170:2153–2157.
24. Reddy JA, Xu LC, Parker N, Vetzel M, Leamon CP. Preclinical evaluation of ^{99m}Tc-EC20 for imaging folate receptor-positive tumors. *J Nucl Med.* 2004;45: 857–866.
25. Morris RT, Joyrich RN, Naumann RW, et al. Phase II study of treatment of advanced ovarian cancer with folate-receptor-targeted therapeutic (vintafolide) and companion SPECT-based imaging agent (^{99m}Tc-etarfolatide). *Ann Oncol.* 2014;25:852–858.
26. Ahlskog JK, Schliemann C, Marlind J, et al. Human monoclonal antibodies targeting carbonic anhydrase IX for the molecular imaging of hypoxic regions in solid tumours. *Br J Cancer.* 2009;101:645–657.
27. Oosterwijk E. Carbonic anhydrase expression in kidney and renal cancer: implications for diagnosis and treatment. *Subcell Biochem.* 2014;75:181–198.
28. Moschetta M, Pretto F, Berndt A, et al. Paclitaxel enhances therapeutic efficacy of the F8-IL2 immunocytokine to EDA-fibronectin-positive metastatic human melanoma xenografts. *Cancer Res.* 2012;72:1814–1824.
29. Haraldsson B, Nystrom J, Deen WM. Properties of the glomerular barrier and mechanisms of proteinuria. *Physiol Rev.* 2008;88:451–487.
30. Zechmann CM, Afshar-Oromieh A, Armor T, et al. Radiation dosimetry and first therapy results with a ^{124}I/^{131}I-labeled small molecule (MIP-1095) targeting PSMA for prostate cancer therapy. *Eur J Nucl Med Mol Imaging.* 2014;41: 1280–1292.
31. Chari RV, Miller ML, Widdison WC. Antibody-drug conjugates: an emerging concept in cancer therapy. *Angew Chem Int Ed Engl.* 2014;53:3796–3827.